A New Efficient Approach for Designing FIR Low-pass Filter and Its Application on ECG Signal for Removal of AWGN Noise

Hrishi Rakshit and Muhammad Ahsan Ullah

Abstract—**In this paper, a new class of adjustable window function, based on combination of tangent hyperbolic function and a weighted cosine series, is proposed to design an FIR filter. The proposed window has only one adjustable parameter "r". By varying this parameter, it is possible to change the spectral characteristics of the filter. The performance of the proposed window is compared with Gaussian and Kaiser windows. The proposed window has slightly larger main–lobe width compare to the commonly used Gaussian and Kaiser windows, while featuring 19.71 dB and 8.29 dB smaller ripple ratios respectively. Moreover the side-lobe roll-off ratio of the proposed window is almost 115.03 dB and 14.95 dB better than the Gaussian and Kaiser windows respectively. Simulation results show that the filter designed by the proposed window, yields 4.45 dB and 30.69 dB smaller ripple ratios and 7.7 times and 5 times better side-lobe roll-off ratios than those of Gaussian and Kaiser windows respectively. This paper also highlights an application of the proposed method in the area of eliminating noise from corrupted ECG signals.**

Index Terms— **Gaussian Window, Kaiser Window, Main-lobe Width, Ripple Ratio and Side-lobe Roll-off Ratio.**

I. Introduction

The impulse response of an ideal filter is infinitely long. The most straight forward way to make the response finite, is to truncate the ideal response. If $h_d(n)$ is the response of an ideal filter, the simplest way to obtain a causal finite impulse response is to multiply the $h_d(n)$ with a finite window function w(n). In engineering term, a window is a finite array, consists of coefficients to satisfy the desirable requirements [1]. In general, the window function can be defined as

$$w[n] = \begin{vmatrix} f(n), & 0 \le n \le N \\ 0, & otherwise \end{vmatrix} \quad (1)$$

and the impulse response of the system is given by

$$h[n] = h_d[n]w[n] \quad (2)$$

Manuscript received July 17, 2015; revised March 03, 2016. Hrishi Rakshit is with the Department of Electrical and Electronic Engineering, Chittagong University of Engineering and Technology (CUET), Chittagong – 4349, Member of IAENG, Member Number: 166484. Bangladesh phone:+88-01818-855141; e-mail: rishirok@ gmail.com).

Muhammad Ahsan Ullah is with the Department of Electrical and Electronic Engineering, Chittagong University of Engineering and Technology (CUET), Chittagong – 4349, Bangladesh phone:+88-01734-311590; e-mail: ahsan_cuet@ yahoo.com).

Therefore the Fourier transform h[n], denoted by $H(e^{j\omega})$, is the periodic convolution of the $H_d(e^{j\omega})$, with the Fourier transform of w[n], denoted by $W(e^{j\omega})$. The important spectral characteristics of a window function are i) main-lobe width ii) ripple ratio and iii) its side-lobe roll-off ratio. There are two desirable specifications for any window function. They are smaller main-lobe width and the smaller ripple ratio. However, these two requirements are contradictory [2]. The simplest window is the rectangular window [2].It has a very sharp transition band. The ripple ratio of the rectangular window is higher than any other established window. Gaussian and Kaiser windows are the adjustable functions. So by changing the adjustable parameter, optimization between the main-lobe width and the ripple ratio can be made on Gaussian and Kaiser windows. In many applications like FIR filters, FFT, signal processing and measurements, we are required -45 dB or less side lobe peaks [3]. Kaiser window has the computational complexity due to the calculation of Bessel functions [4]. So there has been a great interest to design a new window to meet the desire specifications for different applications.

In this paper, a novel adjustable window is proposed which has only two parameters (one is length of the window and another is the additional parameter "r") that control the spectral characteristics of the window. The proposed window is very simple as it does not involve any Bessel function like the Kaiser window. The proposed window yields better spectral characteristics than Gaussian window. The ripple ratio and the side-lobe roll-off ratio of the proposed window are 19.71 dB and 115.03 dB better than those of the Gaussian window. Our simulation results confirm that the ripple ratio and the side-lobe rill-off ratio of the proposed window are 8.29 dB and 14.95 dB better respectively than what can be obtained using Kaiser window. Filter designed using the proposed window results 4.45 dB and 30.69 dB better ripple ratios than Gaussian and Kaiser windows respectively. Moreover, the side-lobe roll-off ratio of the proposed window based FIR low-pass filter is 7.7 times and 5 times greater than the mentioned named windows based filters respectively. The filter, designed by the proposed method, has been used to remove noise from

(Advance online publication: 18 May 2016)

corrupted ECG signal. The experimental results ensure that the proposed filter performs better performance than Gaussian and Kaiser filters to eliminate noise from ECG signal.

Section II defines the three major spectral characteristics of a window function. Section III introduces the new window and also explains its spectral behaviors under various conditions. Section IV compares the performances of the proposed window with Gaussian and Kaiser windows. Section V describes the performance analysis of a FIR low-pass filter using the proposed windowing method. Section VI represents the efficiency of the proposed FIR low-pass filter in eliminating noise from the corrupted ECG signal. Section VII shows the normalized frequency response of the filtered ECG signal. Section VIII provides concluding remarks.

II. Spectral properties of Windows

A window, w(nT), with a length of N is a time domain function which is nonzero co-efficient for n<=|(N-1)/2| and zero for otherwise. A typical window has a normalized amplitude spectrum in dB as shown in Figure 1.

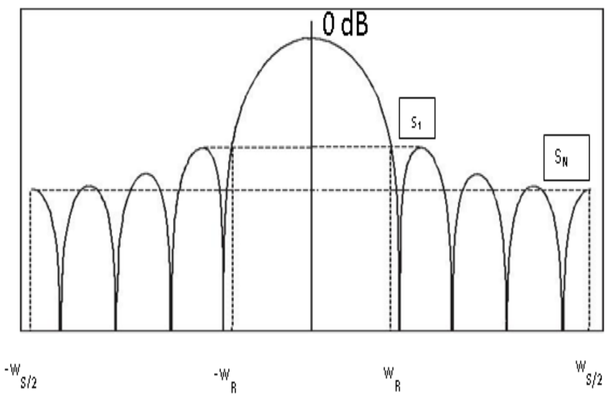

Fig 1: A typical window's normalized amplitude spectrum

Normalized spectrum in Fig1 is obtained by following equation

$$|W_n(e^{j\omega T})| = 20\log_{10}\left(\frac{|A(w)|}{|A(w)|_{\max}}\right) \quad (3)$$

The spectral characteristics which determine the windows performance are the main-lobe width(w_M), the ripple ratio (R) and the side-lobe roll-off ratio(S). From the Fig. 1, these parameters can be defined as

W_M= Two times half of the main-lobe width=$2w_R$.

R= (Maximum side-lobe amplitude in dB) – (Main-lobe amplitude in dB) = S_1.

S= (Maximum side-lobe amplitude in dB) – (Minimum side-lobe amplitude in dB) = S_1-S_N.

III. Proposed Window

The new proposed window is a combination of tangent hyperbolic function and a weighted cosine series. The tan hyperbolic function is given by the following equation

$$y_1 = \left[\tanh\left\{\frac{n - \frac{(N-1)}{2} + \cosh^2(\alpha)}{B}\right\} - \tanh\left\{\frac{n - \frac{(N-1)}{2} - \cosh^2(\alpha)}{B}\right\}\right] \quad (4)$$

The weighted cosine function is expressed as follows

$$y_2 = 0.375 - 0.5\cos\left\{\frac{2\pi l}{N-1}\right\} + 0.125\cos\left\{\frac{4\pi l}{N-1}\right\} \quad (5)$$

where N is the length of the window, α and B are the constants. Here 'n' is the number of samples. Here the symbol l =0,1,2,3,……(N-1).

These two equations are combined in the following way.

$$w(n) = (y_1 * y_2)^{\gamma}, \quad where, \gamma = r^{(\frac{1}{5})} \quad (6)$$

and "*" means multiplication.

Here r is a variable which controls the shape and the frequency response of the window. So "r" can be named as controlling or adjustable parameter of the window. In mathematical term, the window can be expressed as

$$w(n) = \begin{vmatrix} (y_1 * y_2)^{\gamma}, & n \le 0 \le N \\ 0, & otherwise \end{vmatrix} \quad (7)$$

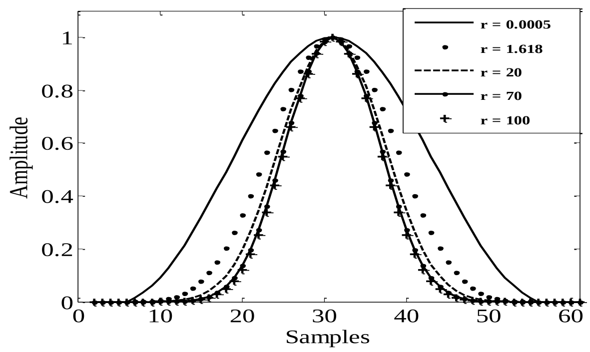

Fig 2: Shapes of the proposed windows with different values of r.

From the Fig 2 it has been observed that the shape of the window varies as the value of the adjusting parameter "r" changes. When r=0.0005 and r =100, the shape of the window is the widest and the narrowest respectively among the other values of "r" shown in the Fig 2. The width of the window gets narrower as the value of the controlling parameter "r" gets bigger.

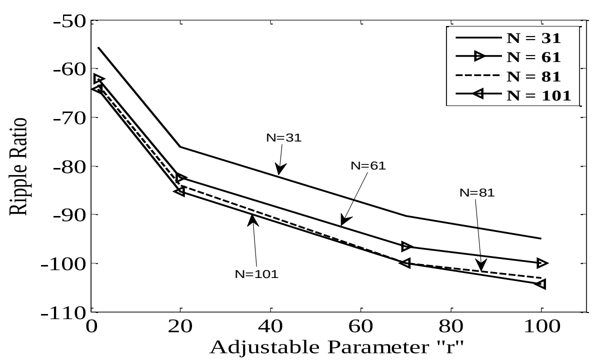

Fig 3 : Adjustable parameter "r" Vs Ripple ratio curve in different window lengths

In the Fig 3, the curve N=31 describes the ripple ratios of different values of "r" when the window length is fixed at 31. In the same way, N=61, N=81 and N=101 curves have been drawn. It has been observed from Fig 3 that the ripple ratio decreases with the increment of "r" when the window length is fixed. Among all the curves in Fig 3, N=101 shows better performance in terms of ripple ratio calculation. The following table summarizes the Fig 3.

TABLE I: ADJUSTABLE PARAMETER VS. RIPPLE RATIO AT VARIOUS WINDOW LENGTH N.

Adjustable Parameter	Ripple Ratio at Different Window Length			
"r"	N=31	N=61	N=81	N=101
0.0005	-25.7	-33.2	-31.84	-33.36
1.618	-55.68	-62.1	-63.31	-64.27
20	-76.16	-82.47	-84.1	-85.28
70	-90.28	-96.58	-100	-100
100	-94.92	-100	-103.1	-104.4

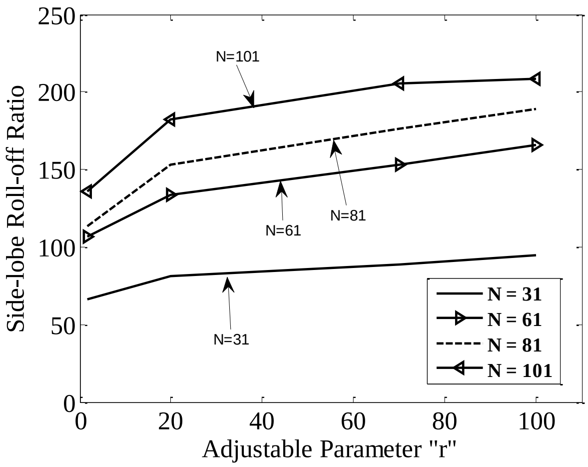

Fig4 : Adjustable parameter "r" Vs. Side-lobe roll-off ratio curve in different window lengths.

From the Fig 4 it has been observed that all the curves are increasing with the increment of the adjustable parameter "r". So it can be said that the side-lobe roll-off ratio of the proposed window increases with the raise of the value of "r" when the window length is fixed. Let us consider the curve N=101. Here N is the window length. Compare to the curve N=31, N=61 and N=81, the curve N=101 remains on the highest position. The following table summarized the Fig 4.

TABLE II: ADJUSTABLE PARAMETER "R" VS SIDE-LOBE ROLL-OFF RATIO AT VARIOUS WINDOW LENGTHS

Adjustable Parameter	Side-lobe Roll-off Ratio at Different Window Length			
"r"	N=31	N=61	N=81	N=101
0.0005	27.09	38.54	40.39	80.64
1.618	66.42	106.9	113.29	135.73
20	81.44	133.33	152.7	182.32
70	88.52	153.42	176.3	205.4
100	94.78	166.1	189.3	208.5

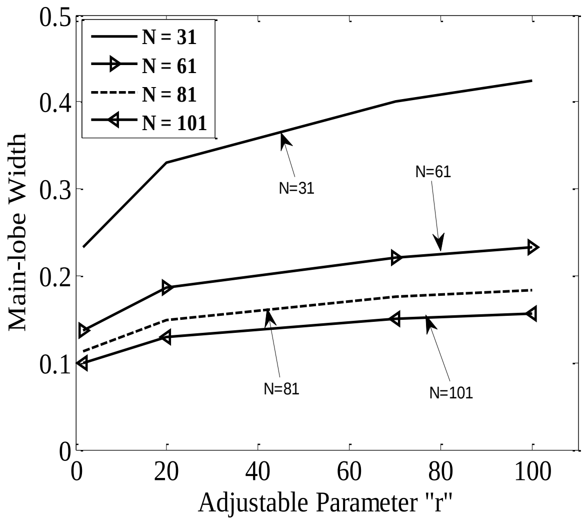

Fig 5 : Adjustable parameter "r" Vs. Main-lobe width curve in different window lengths.

Fig 5 shows that as the controlling parameter of the proposed window "r" increases the main-lobe width of the proposed window also raises when the window length is fixed. Here N is length of the proposed window. From Fig 5 we have noticed that the curve N=101, results better performance among all the curves in Fig 5 in terms of main-lobe width calculation. The following table gives the actual scenario of Fig 5.

TABLE III: ADJUSTABLE PARAMETER "R" VS MAIN-LOBE WIDTH CALCULATION AT VARIOUS WINDOW LENGTHS

Adjustable Parameter	Main-lobe width at Different Window Length			
"r"	N=31	N=61	N=81	N=101
0.0005	0.1096	0.07632	0.06654	0.06262
1.618	0.2329	0.137	0.1135	0.1
20	0.3307	0.1869	0.1487	0.1292
70	0.4	0.2211	0.1761	0.1507
100	0.4247	0.2329	0.184	0.1566

IV. PERFORMANCE ANALYSIS

In this section, we compare the shape and the spectral characteristics of the proposed window with several commonly used windows.

A. *Gaussian Window:*

The coefficients of the Gaussian window function are computed using the following equation.

$$w(n) = e^{\frac{1}{2}\left(\alpha \frac{n}{N/2}\right)^2} \quad (8)$$

where α is inversely proportional to the standard deviation of a Gaussian random variable. The width of the window is inversely related to the value of α. A larger value of α produces a narrower window[5][6].

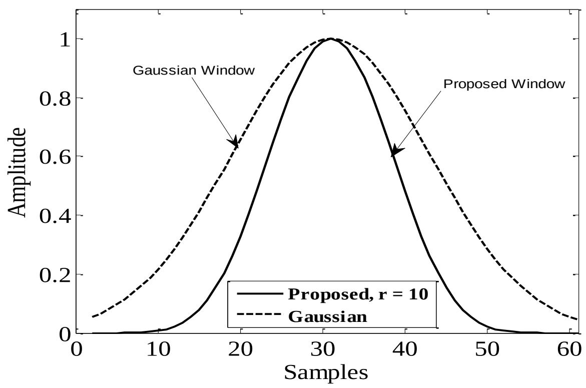

Fig 6: Time domain representation of Gaussian and the Proposed windows

From the Fig 6 it has been noticed that the time domain representation of the proposed window with r =10, is narrower than the Gaussian window. Moreover, the proposed window touches the X-axis while all the coefficients of the Gaussian window remain above the X-axis. Hence the coefficients of the Gaussian window are always greater than zero. On the other-hand, the coefficients of the proposed window evenly touch the X-axis.

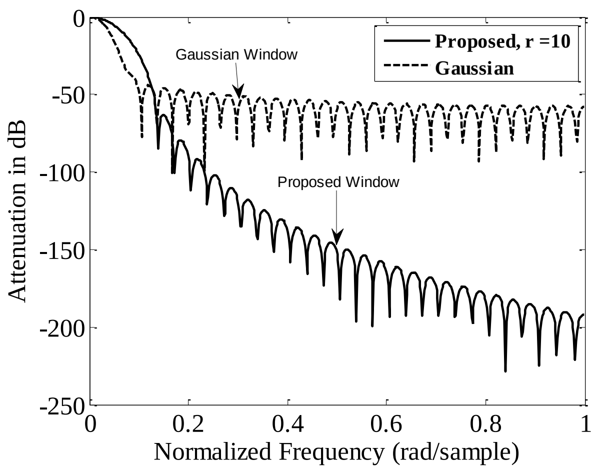

Fig 7: Normalized frequency response comparison of Gaussian and the Proposed windows.

Fig 7 shows that the main lobe width of Gaussian and the proposed windows are 2π × 0.1055 rad/sample and 2π × 0.1387 rad/sample respectively. So the main-lobe width of Gaussian window is 0.0332 rad/sample smaller than the proposed window. On the contrary, the ripple ratio of Gaussian and the proposed windows are about -44.16 dB and -63.83 dB respectively. Hence the ripple ratio of the proposed window is approximately 19.67 dB smaller. Moreover, the side-lobe roll-off ratio of the proposed window is almost 128.47 dB. The Gaussian window results 13.44 dB side-lobe roll-off ratio. Therefore, the proposed window yields 115.03 dB better side-lobe roll-off ratio than Gaussian window.

TABLE IV: SPECTRAL PARAMETERS OF GAUSSIAN AND THE PROPOSED WINDOWS.

Window	Main-lobe Width (rad/sample)	Ripple Ratio (dB)	Side-lobe Roll-off Ratio(dB)
Proposed, r =10	2π × 0.1387	-63.83	128.47
Gaussian	2π×0.1055	-44.12	13.44

B. Kaiser window:

The Kaiser window is also known as Kaiser-Bessel window function. The Kaiser window function can be expressed as follows [7][8].

$$w(n) = \frac{I_0(\pi\alpha\sqrt{1-(\frac{2n}{N-1}-1)^2})}{I_0(\pi\alpha)}\ where, 0 \le n \le N \quad (9)$$

where I_0 is the zero-th order modified Bessel function of the first kind [8]. Kaiser window is another very popular adjustable window. The variable parameter α determines the tradeoff between the main-lobe width and the side lobe attenuation.

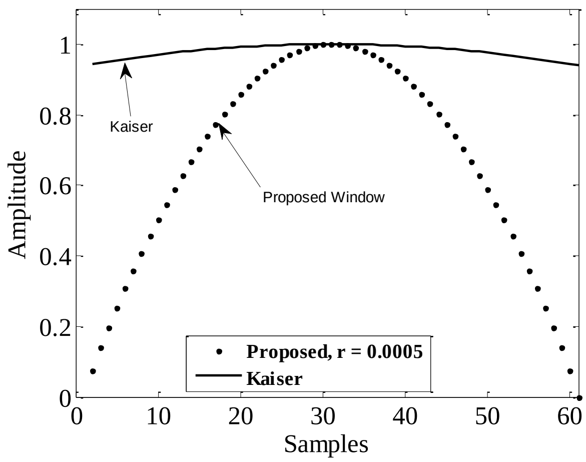

Fig 8 : Time domain representation of Kaiser and the Proposed windows

From the Fig 8 it has been observed that Kaiser window with its adjustable parameter α = 0.5 is almost like rectangular shape. On the contrary, the proposed window is almost like bell shape with its adjustable parameter r= 0.0005.

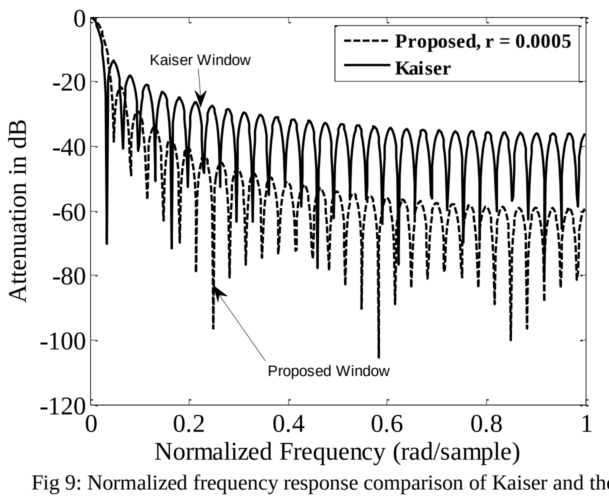

Fig 9: Normalized frequency response comparison of Kaiser and the Proposed windows.

Fig 9 shows the normalized frequency response of Kaiser and the proposed windows. It has been observed that Kaiser window has the main-lobe width of 2π×0.0332 rad/sample while the proposed window has 2π×0.0469 rad/sample. So Kaiser window is slightly better than the proposed window in main-lobe width consideration. Kaiser window has the ripple ratio of -13.63 dB and the proposed window has the ripple ratio of -21.92 dB. Hence the proposed window yields

8.29 dB better ripple ratio than the Kaiser window. Fig 9 illustrates that the first side-lobe peak of Kaiser window is -13.63 dB and the last one is -36.07dB. So the side-lobe roll-off ratio of Kaiser window is 22.44 dB. In the same way, the first side-lobe peak of the proposed window is -21.92 dB and the last one is -59.31 dB. Hence, the side-lobe roll-off ratio of the proposed window is 37.39 dB which is 14.95 dB better than Kaiser window.

TABLE V: SPECTRAL PARAMETERS OF KAISER AND THE PROPOSED WINDOWS.

Window	Main-lobe Width (rad/sample)	Ripple Ratio (dB)	Side-lobe Roll-off Ratio(dB)
Proposed, r =0.0005	2π×0.0469	-21.92	37.39
Kaiser	2π×0.0332	-13.63	22.44

V. FIR FILTER DESIGN:

In this section we will discuss how the proposed window helps us to design FIR low pass filter and also compare the simulation result with the most popular adjustable windows.

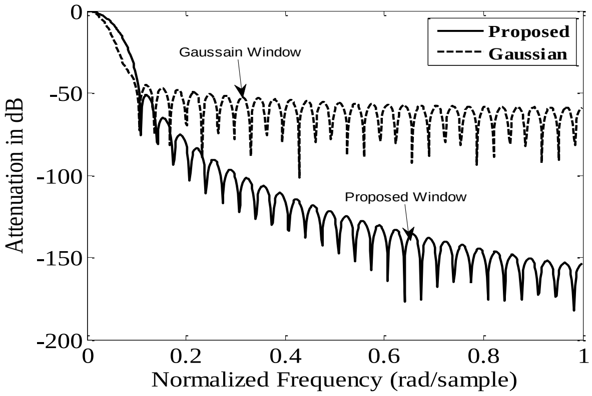

Fig 10 (a) : Normalized frequency response of FIR low pass filters designed by the proposed and Gaussian windows.

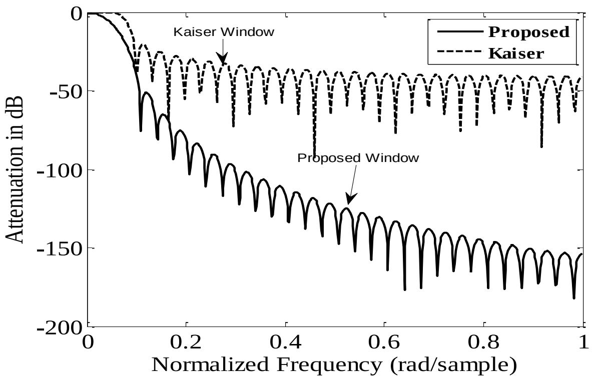

Fig 10 (b) : Normalized frequency response of FIR low pass filters designed by the proposed and Kaiser windows.

Having a cut off frequency of ω_c, the impulse response of an ideal low pass filter is given by

$$h_{LP,ideal}[n] = \frac{\sin(\omega_c n)}{\pi n} \qquad (10)$$

By windowing this IIR filter with the windows discussed in this paper, different FIR filter can be achieved. For $\omega_c = 0.1\pi$ figures 10(a)-10(b) show the normalized frequency response of the FIR filters designed by applying different windows of length 61. Fig 10(a) shows the comparison of FIR low-pass filters designed by the proposed and Gaussian windows respectively. From the Fig 10 (a) it has been observed that the main-lobe width of the proposed window and Gaussian window based FIR low-pass filters are almost the same. Simulation result shows that the filter achieved by the proposed window has 4.45 dB less ripple ratio than what can be obtained by using Gaussian window. Fig 10(a) also depicts that the side-lobe roll-off ratio of the filter, designed by the proposed window is approximately 89.92 dB better than what can be achieved by Gaussian window. In the same way, the fig 10(b) demonstrates that the filter, obtained by the proposed window results 30.69 dB better ripple ratio and approximately 81.83 dB greater side-lobe roll-off ratio than what can be obtained by using Kaiser window. Therefore, the proposed window based FIR low-pass filter performs better performance than Gaussian window and Kaiser window based FIR low-pass filters with the same window length.

TABLE V: DATA ANALYSIS OF FIR FILTER OBTAINED BY WINDOWING WITH DIFFERENT WINDOWS

Comparing Windows	Main-lobe Width (rad/sample)	Ripple Ratio (dB)	Side-lobe Roll-off Ratio (dB)
Proposed Vs Gaussian	2π×0.1074	-49.94	103.26
	2π×0.1074	-45.49	13.34
Proposed Vs Kaiser	2π×0.1094	-51.36	102.04
	2π×0.0977	-20.67	20.21

VI. Noise Elimination from ECG signal

The electrical activity of heart is called ECG signal which is generated by repolarization and depolarization of the atria and ventricles [9]. The ECG signals are very small in amplitude. The frequency range of the ECG signal lies in between 0.05 to 100 Hz. ECG signal is invasively recorded using surface electrodes on the limbs and chest [12]. ECG signals are consist of P-waves, QRS complex and T-waves. The depolarization of atria results P-waves [8]. The QRS complex consists of three waves, sequentially Q, R and S waves. The rapid depolarization of both the ventricles yields the QRS complex. Ventricular repolarization generates T-waves [10]. The standard ECG signal of one period is shown in the Fig 11. Arti-factual signals are generated from various internal and external sources and mixed with ECG signal. The noise generally caused by the signal from muscle contractions, which can be expressed as zero mean Gaussian noise [11].

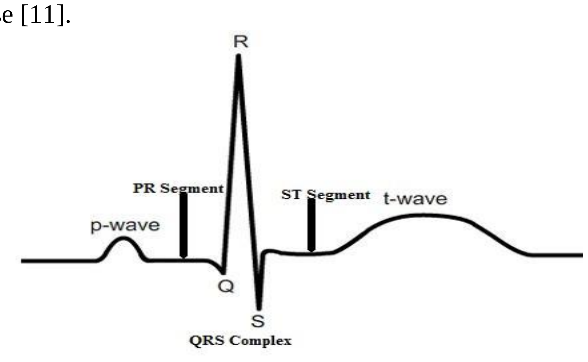

Fig 11: Typical ECG trace.

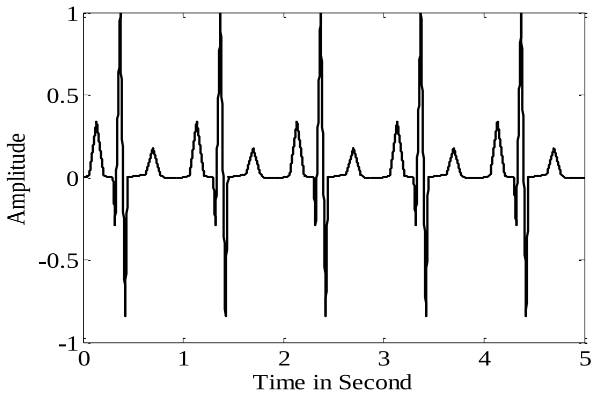

Fig 12: Noiseless heart signal

Fig 12 shows a simulated version of noiseless heart signal. Now if this ECG signal is corrupted by Additive White Gaussian Noise, then the view of the ECG signal becomes as below.

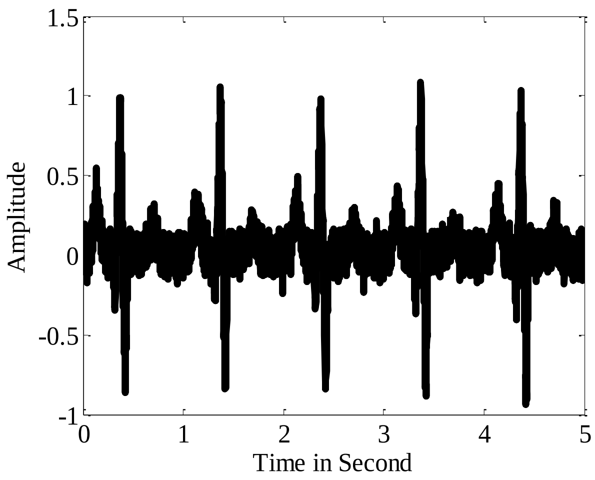

Fig 13: Corrupted ECG signal due to Additive White Gaussian Noise

This corrupted ECG signal is then passed through a low pass FIR filter which is designed using Gaussian window function. The result is shown in the Fig 14.

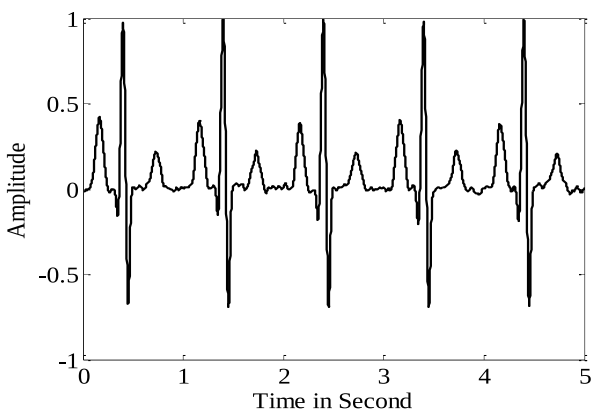

Fig 14: Filtered ECG signal using Gaussian window based FIR low pass filter

The same corrupted ECG signal is then passed through another FIR low pass filter which is designed using Kaiser window function. The result is shown in the Fig 15.

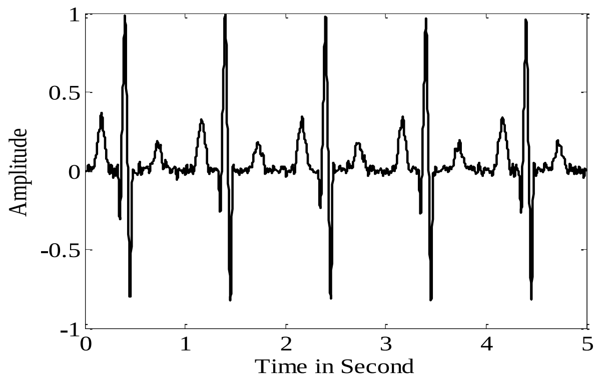

Fig 15: Filtered ECG signal using Kaiser window based FIR low pass filter

Now the additive white Gaussian noise corrupted ECG signal is given to the input of the proposed window based FIR low-pass filter. At the output, the following figure is found.

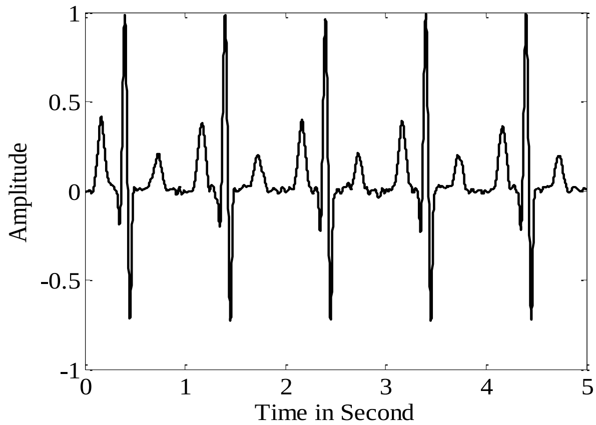

Fig 16: Filtered ECG signal using the Proposed window based FIR low pass filter

We have observed that the P and R peaks are sharper in Fig 16 than those of Fig 14 and Fig 15. Moreover the QRS complexes are more clearly traceable in Fig 16 rather than Fig 13 and Fig 14. Now to calculate how precisely the above filters eliminate noise from the corrupted ECG signal, cross-correlation is introduced here to correlate each filter output with the original or noiseless ECG signal. In that case, the percentage of similarities of each filter output to the original noiseless ECG signal has been measured. The following table shows the cross-correlation of each filter output to the original ECG signal.

TABLE VI: CORRELATION PERCENTAGE OF FILTERED SIGNALS TO ORIGINAL SIGNAL

Filter Name	Correlation Percentages
Gaussian Filter	75.18%
Kaiser Filter	73.07%
Proposed Filter	80.44%

Table VI shows that the proposed filter eliminates noise from the corrupted ECG signal more precisely than the Gaussian and the Kaiser filters.

VII. Normalized Frequency response of ECG signal

After obtaining the filtered version of the ECG signal using Gaussian, Kaiser and the proposed windows based FIR low-pass filters, their respective normalized frequency response has been analyzed. The frequency range of an ECG signal ranges from 0.05 to 120 HZ. Fig17, Fig 18 and Fig19 show the normalized frequency response of the ECG signal filtered by Gaussian, Kaiser and the proposed windows based FIR filters respectively.

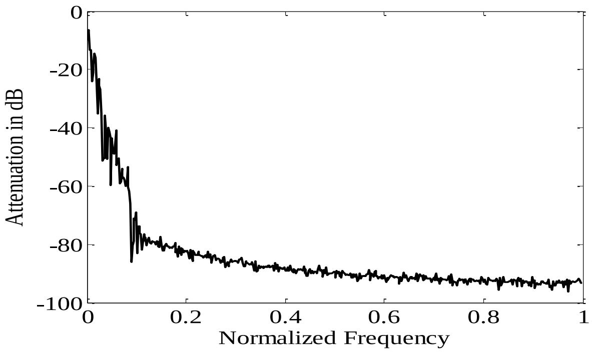

Fig17: Normalized frequency response of the filtered ECG signal using Gaussian window based FIR low-pass filter.

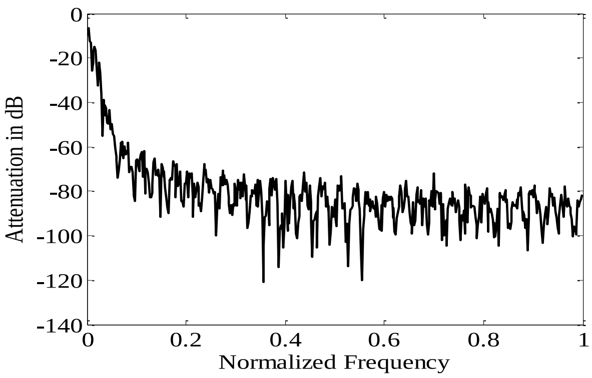

Fig 18: Normalized frequency response of the filtered ECG signal using Kaiser window based FIR low-pass filter.

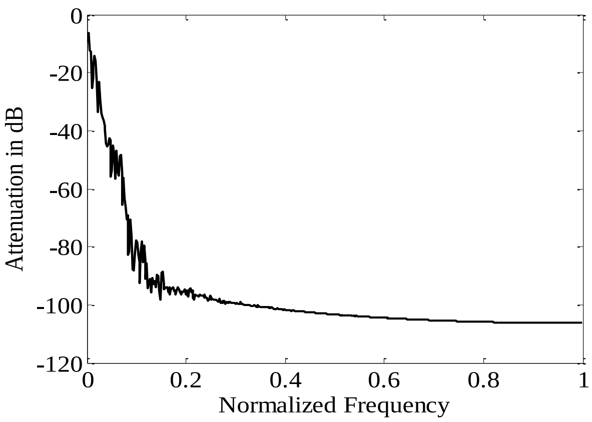

Fig 19: Normalized frequency response of the filtered ECG signal using proposed window based FIR low-pass filter

Fig 17 shows that the ripple ratio of the filtered ECG signal, using Gaussian filter and it is -69.08 dB. It has been observed from Fig 18 that the ripple ratio of the filtered ECG signal using Kaiser low-pass filter is -65.69 dB. The ripple ratio of the filtered ECG signal filtered by the proposed window based FIR low-pass filter is -78.57 dB. Hence the proposed window based FIR filter achieves 9.49 dB and 12.88 dB better performances in terms of ripple ratio calculation compare to the Gaussian and the Kaiser filters within the frequency range of the ECG signal. The side-lobe roll-off ratio of the filtered ECG signal, obtained by the proposed method, is 4.84 dB and 11.8 dB better than the Gaussian and the Kaiser filters respectively.

TABLE VII: SPECTRAL CHARACTERISTICS OF ECG SIGNAL FILTERED BY DIFFERENT FILTERS

Filter	Ripple ratio in dB	Side-lobe roll-off ratio in dB
Gaussian	-69.08	22.73
Kaiser	-65.69	15.77
Proposed	-78.57	27.57

VIII. Conclusion

The proposed window is symmetric one and it has only one adjustable parameter “r”. So it is a very simple window. The performance of the FIR low pass filter, designed by the proposed window, is compared with Gaussian and Kaiser windows. Experimental results show that the filter designed by the proposed window yields 4.45 dB and 30.69 dB smaller ripple ratios and approximately 7.7 times and 5 times better side-lobe roll-off ratio than those of Gaussian and Kaiser windows respectively. The paper has also shown that the proposed filtering method can be used to achieve 9.49 dB and 12.88 dB improved ripple ratio compared to Gaussian and Kaiser filtering methods to eliminate noise from ECG signals. Moreover, the proposed filter eliminates AWGN noise more precisely from the corrupted ECG signal than the Gaussian and the Kaiser filtering methods. At the same time, the side-lobe roll-off ratio of the filtered ECG signal, filtered by the proposed method, is 4.84 and 11.8 dB better than those of the Gaussian and the Kaiser filtering methods respectively.

REFERENCES

[1] Hrishi Rakshit and Muhammad Ahsan Ullah “A Comparative Study on Window Functions for Designing Efficient FIR Filter”. In Proceedings of the IEEE 9th International Forum on Strategic Technology (IFOST), ISBN: 978-1-4799-6060-6 DOI: 10.1109/IFOST.2014.6991079 pp 91-96, 2014.

[2] Oppenheim, A.V., and R.W. Schafer. Discrete-Time Signal Processing. Upper Saddle River, NJ: Prentice-Hall, 1999, pp. 468-471..

[3] Md abdus Samad “A Novel Window Function Yielding Suppressed Main-lobe Width and Minimum Side-lobe Peak” International Journal of Computer Science, Engineering and Information technology (IJCSEIT), Vol 2, No 2, April 2012.

[4] Emmanuel C. Ifeacher and Barrie W. Jervis “Digital Signal Processing” second edition, Pearson Education 2008.

[5] Roberts, Richard A., and C.T. Mullis. Digital Signal Processing. Reading, MA: Addison-Wesley, 1987, pp. 135-136.

[6] Harris, F.J. "On the Use of Windows for Harmonic Analysis with the Discrete Fourier Transform." Proceedings of the IEEE. Vol. 66, No. 1 (January 1978).

[7] Kaiser, J.; Schafer, R. (1980). "On the use of the I0-sinh window for spectrum analysis". IEEE Transactions on Acoustics, Speech, and Signal Processing 28: 105.

[8] Selected Papers in Digital Signal Processing II, IEEE Press, New York, 1975.

[9] AK.M Fazlul Haque, Md. Hanif Ali, M. Adman Kiber, Md. Tanvir Hasan,”Detection of small variations of ECG features using Wavelets”. ARPN ,Journal of Engineering and Applied Science, ISSN 1819-6608, Vol. 4,No. 6, pp.27-30,Aug2009.

[10] Smith, SW. “Atrial Repolarization Wave Mimicking ST Depression ” Retrieved 22 October 2014.

[11] S.A. Chouakri, F. Bereksi-Reguig, S. Ahamaidi, and O. Fokapu, “Wavelet de-noising for the Electrocardiogram signal based on the corrupted noise estimation” Computers in Cardiology, pp. 1021-1024, 2005.
[12] J. Jenitta A. Rajeswari “An optimized Baseline Wander Removal Algorithm Based on Ensemble Empirical Mode Decomposition”, IAENG International Journal of Computer Science, vol.42, no.2, pp 95-106, 2015.